Applied Surface Science 341 (2015) 100–108

Contents lists available at ScienceDirect

Applied Surface Science

journal homepage: www.elsevier.com/locate/apsusc

CH_4 dehydrogenation on Cu(1 1 1), Cu@Cu(1 1 1), Rh@Cu(1 1 1) and RhCu(1 1 1) surfaces: A comparison studies of catalytic activity

Riguang Zhang[a], Tian Duan[a], Lixia Ling[a,b], Baojun Wang[a,*]

[a] Key Laboratory of Coal Science and Technology of Ministry of Education and Shanxi Province, Taiyuan University of Technology, Taiyuan 030024, Shanxi, P.R. China

[b] Research Institute of Special Chemicals, Taiyuan University of Technology, Taiyuan 030024, Shanxi, P.R. China

ARTICLE INFO

Article history:
Received 13 January 2015
Received in revised form 3 March 2015
Accepted 3 March 2015
Available online 9 March 2015

Keywords:
Methane
Dehydrogenation
Cu-based Catalyst
Rhodium
Density functional theory

ABSTRACT

In the CVD growth of graphene, the reaction barriers of the dehydrogenation for hydrocarbon molecules directly decide the graphene CVD growth temperature. In this study, density functional theory method has been employed to comparatively probe into CH_4 dehydrogenation on four types of Cu(1 1 1) surface, including the flat Cu(1 1 1) surface (labeled as Cu(1 1 1)) and the Cu(1 1 1) surface with one surface Cu atom substituted by one Rh atom (labeled as RhCu(1 1 1)), as well as the Cu(1 1 1) surface with one Cu or Rh adatom (labeled as Cu@Cu(1 1 1) and Rh@Cu(1 1 1), respectively). Our results show that the highest barrier of the whole CH_4 dehydrogenation process is remarkably reduced from 448.7 and 418.4 kJ mol^{-1} on the flat Cu(1 1 1) and Cu@Cu(1 1 1) surfaces to 258.9 kJ mol^{-1} on RhCu(1 1 1) surface, and to 180.0 kJ mol^{-1} on Rh@Cu(1 1 1) surface, indicating that the adsorbed or substituted Rh atom on Cu catalyst can exhibit better catalytic activity for CH_4 complete dehydrogenation; meanwhile, since the differences for the highest barrier between Cu@Cu(1 1 1) and Cu(1 1 1) surfaces are smaller, the catalytic behaviors of Cu@Cu(1 1 1) surface are very close to the flat Cu(1 1 1) surface, suggesting that the morphology of Cu substrate does not obviously affect the dehydrogenation of CH_4, which accords with the reported experimental observations. As a result, the adsorbed or substituted Rh atom on Cu catalyst exhibit a better catalytic activity for CH_4 dehydrogenation compared to the pure Cu catalyst, especially on Rh-adsorbed Cu catalyst, we can conclude that the potential of synthesizing high-quality graphene with the help of Rh on Cu foils may be carried out at relatively low temperatures. Meanwhile, the adsorbed Rh atom is the reaction active center, namely, the CVD growth can be controlled by manipulating the graphene nucleation position.

1. Introduction

Chemical vapor deposition (CVD) has been widely used in graphene synthesis with many different metals as the substrate [1–3]. Among them, Ni has good lattice match with graphene, while Cu is superior for controllably growing single layer graphene [2,4]. An isotope-effect study indicates that, during CVD growth of graphene on Ni substrate, carbon atoms dissolve into the bulk. Contrarily, the growth process is limited on the surface in the Cu case [5], which makes Cu become the most popular CVD substrates for graphene growth. In the growth process of graphene, the reaction barriers for the dehydrogenation of hydrocarbon molecules directly decide the graphene CVD growth temperature, and the dissociative C atoms tend to accumulate at the dehydrogenation reaction centers [6]. Accordingly, the sequence of CH_4 dehydrogenation reactions that transform CH_4 into C and H on catalyst surfaces are also often regarded as the crucial steps for the productions of graphene, carbon nanotubes and carbon nanofibers by CVD method [5,7,8]. As a result, the fundamental insight into the CH_4 dehydrogenation on Cu substrate for the CVD growth of graphene at the molecular level is essential for understanding and clarifying the dehydrogenation process. Indeed, complete dehydrogenation behaviors of CH_4 on metal Cu substrates have been studied theoretically, for example, Zhang et al. [5] have investigated CH_4 complete dehydrogenation on Cu(1 0 0) substrate, suggesting that carbon atoms are thermodynamically unfavorable on a Cu surface under typical experimental conditions, and the active species for graphene growth should thus mainly be CH_x instead of atomic carbon. Wang et al. [6] have investigated CH_4 complete dehydrogenation on metal Cu(1 0 0) and Cu@Cu(1 0 0) substrates. In addition, Wang et al. [9] and Liao et al. [10] have investigated CH_4 complete dehydrogenation on Cu(1 1 1) substrates.

On the other hand, tuning the relative barrier of the different steps of CH_4 dehydrogenation by doping or adsorbing active

* Corresponding authorTel.: +86 351 6018239; fax: +86 351 6041237.
E-mail addresses: wangbaojun@tyut.edu.cn, quantumtyut@126.com (B. Wang).

http://dx.doi.org/10.1016/j.apsusc.2015.03.013
0169-4332/

metallic impurity into the inactive metal would remarkably alter the catalytic activity. For example, previous studies by Wang et al. [6] have revealed that the reaction barriers of CH_4 dehydrogenation on a bimetallic Ni/Cu(1 0 0) surface is much lower than those on the pure Cu(1 0 0) surface. Kokalj et al. [11] have found that the combination of a very active reaction centers such as Rh with a more inactive substrate-such as Cu(1 1 1)-may hinder CH_3 dehydrogenation step with respect to CH_4 dehydrogenation in comparison with those on the pure Rh(1 1 1) surface. Larsen et al. [12] have shown that Co films deposited on Cu(1 1 1) are more reactive that the pure Co itself for CH_4 dehydrogenation. An et al. [13] have revealed that the reaction barriers of CH_4 dehydrogenation on a bimetallic Cu/Ni(1 1 1) surface are much larger than those on the pure Ni(1 1 1). Zhao et al. [14] have investigated the dissociation of CH_4 and CH on Ni(2 1 1) and Pd/Ni(2 1 1) step surfaces, as well as the broad Ni(1 0 0) and Pd/Ni(1 0 0) surfaces, suggesting that Pd-doping Pd/Ni surfaces raises the activation barriers for CH_4 and CH dissociations compared to the pure Ni surface. Thus, on the basis of above studies, it is concluded that the metallic impurity can greatly alter the catalytic activity of the substrate [11].

Nowadays, the case of Rh-decorated Cu catalyst has attracted a large number of studies because of its catalytic activity, such as syngas conversion to ethanol [15], the reactions of CH_x hydrogenation and dehydrogenation, CO insertion into CH_x [16], NO dissociation [17], and CH_4 conversion to ethane [18], and so on. Among these reactions, Rh with more reactivity than Cu is served as the reaction active center on Cu catalyst. Unfortunately, to the best of our knowledge, few studies about CH_4 dehydrogenation on Rh-decorated Cu catalyst at atomic scale have been reported, which might be applied as a basis for the selective modification of Cu substrate to improve the performance towards the CVD growth of graphene.

In this study, encouraged by above reported studies, we have carried out the detailed investigations about CH_4 dehydrogenation by considering a reaction center characterized by a active metallic atom, such as Rh, on a less reactive substrate, such as Cu(1 1 1) involved in the graphene CVD growth. The results are expected to probe into the effect of active metallic impurity on the catalytic activity of Cu-based catalyst for CH_4 dehydrogenation, in which CH_4 dehydrogenation on a pure Cu(1 1 1) surface and a Rh atom substitutionally embedded into Cu(1 1 1) surface (labeled as RhCu(1 1 1)), as well as the Cu(1 1 1) surface with one Cu or Rh adatom (labeled as Cu@Cu(1 1 1) or Ni@Cu(1 1 1), respectively) have been systematically and comparatively investigated by the periodic density functional theory (DFT) method. Such a study is fundamental to gain a comprehensive understanding of CH_4 dehydrogenation on Cu-based substrates, and expected to play an important role to improve the catalytic performance in practical cases for the CVD growth of graphene on Cu-based systems.

2. Computational details

2.1. Calculation method

All calculations have been carried out in the framework of DFT using the Dmol^3 program package in Materials Studio 4.4 [19,20], where the generalized gradient approximation (GGA) corrected the exchange-correlation functional proposed by Perdew-Wang 91 (PW91) [21] is chosen together with the doubled numerical basis set plus polarization basis sets (DNP) [22]. The inner electrons of metal atom are kept frozen and replaced by an effective core potential (ECP) [23,24], and other atoms are treated with an all–electron basis set. For the geometry optimization, the forces imposed on each atom are converged to be less than 0.0004 Ha/Å (1 Ha = 2625.5 kJ mol^{-1}), the total energy converged to be less than 2.0×10^{-5} Ha and the displacement convergence converged to be less than 5×10^{-3} Å, respectively. Brillouin-zone integrations have been performed using $2 \times 2 \times 1$ k-point grid, and a Fermi smearing of 0.005 Ha is used to improve the computational performance.

In order to determine accurate activation barriers of the reaction, we chose Complete LST/QST approach to search for transition states of the reactions [25]. In this method, the linear synchronous transit (LST) maximization is performed, followed by an energy minimization in directions conjugating to the reaction pathway to obtain the approximated TS, which is used to perform quadratic synchronous transit (QST) maximization, then, another conjugated gradient minimization is performed. The cycle is repeated until a stationary point is located. In addition, frequency analysis has been used to validate the transition state corresponding to only one imaginary frequency, and TS confirmation is performed on every transition state to confirm that they lead to the desired reactants and products.

2.2. Surface model

In the surface calculation, the face-center-cubic (1 1 1) surface of close-packed metal Cu, fcc(1 1 1), has been employed to investigate the catalytic activity of CH_4 complete dehydrogenation. The choice of (1 1 1) surface is motivated by two factors: (i) experimentally, both Cu(1 0 0) and (1 1 1) surfaces can promote the CVD growth of graphene [26,27]; (ii) Cu(1 1 1) surface is the most thermodynamically stable Cu facet [28,29].

Cu(1 1 1) surface is represented by a three-layer slab, periodically repeated in a super cell geometry with a 10 Å vacuum slab between any successive metal slabs. To accommodate the larger coadsorbed species without the significant lateral interaction across the repeated unit cells, we employ a $p(4 \times 4)$ unit cell corresponding to a 1/16 monolayer (ML) coverage for each single adsorbate. Since surface relaxation effects of Cu system are small [30–32], the bottom layer is constrained at the bulk position in order to mimic the presence of a larger number of layers in real metal particles, whereas the upper two layers together with the adsorbed species involved in CH_4 dehydrogenation are allowed to relax.

On the other hand, in order to investigate the effect of metal impurity on the catalytic activity of Cu catalyst for CH_4 dehydrogenation, three types of other Cu surfaces have been constructed; firstly, one surface Cu atom in Cu(1 1 1) is substituted by one Rh atom, this surface will henceforth be referred to as RhCu(1 1 1). Secondly, adsorbing one Cu or Rh atom on the first layer of Cu(1 1 1) surface are considered, which are donated as the Cu@Cu(1 1 1) and

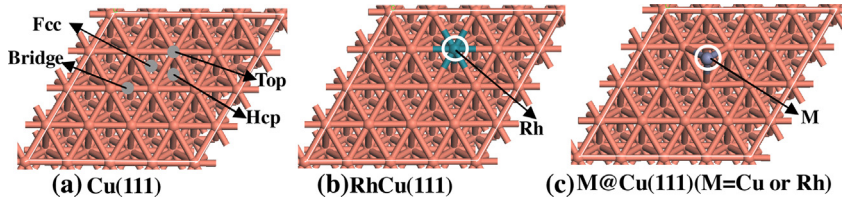

Fig. 1. The top view of (a) Cu(1 1 1), (b) RhCu(1 1 1), and (c) M@Cu(1 1 1)(M = Cu or Rh) surfaces, respectively.

Rh@Cu(1 1 1) surfaces, respectively. All other parameters are the same with Cu(1 1 1) surface. All parameters defining the numerical accuracy of the calculations are carefully tested and well converged. In addition, above three-layer model has been widely used in the previous studies of ethanol oxidation, decomposition, and synthesis, as well as methanol synthesis [33–37]. As shown in Fig. 1, four different adsorption sites exist on these surfaces: Top, Bridge, Hcp, and Fcc.

3. Results and discussion

In order to verify the reliability of the selected calculation methods, we first calculate the lattice constant of bulk Cu (3.682 Å), which is close to the experimental value of 3.615 Å [38], as well as other similar GGA results [28]. Then, the next test is to obtain the bond length and bond angle of CH_4, both are $r_{(C-H)} = 1.094$ Å and $\theta_{(H-C-H)} = 109.5^\circ$, respectively, which agrees with the experimental values of 1.096 Å and 109.4° [39]. These test results show that the calculated method employed in this study is reliable.

3.1. The stability of the different Cu surfaces

The stability of Cu catalyst surface is determined by its formation energy (E_f) as follows:

$$E_f = E_{M/Cu,slab} + E_{Cu,atom} - E_{Cu,slab} - E_{M,atom}$$

Where $E_{M/Cu,slab}$ and $E_{Cu,slab}$ are the total energies of the M/Cu and pure Cu surface, and $E_{M,atom}$ and $E_{Cu,atom}$ are the single metal M atom (M = Cu or Rh). A negative value for E_f indicates that the formation of M/Cu surface from the corresponding Cu surface is exothermic, as a result, the resulting M/Cu surface is relatively stable.

Our results show that for Cu@Cu(1 1 1) and Rh@Cu(1 1 1) surfaces, the single Cu or Rh atom is stably adsorbed at the three-fold hollow site (fcc) on Cu(1 1 1) surface, the formation of these two surfaces is exothermic by 264.8 and 1235.2 kJ mol^{-1}, respectively; for RhCu(1 1 1) surface, the formation is exothermic by 1374.8 kJ mol^{-1}; in addition, the energy needed for a Cu atom removed from the pure Cu(1 1 1) surface leading to the defective surface is 366.8 kJ mol^{-1}. Thus, Cu@Cu(1 1 1), Rh@Cu(1 1 1) and RhCu(1 1 1) surfaces are all relatively stable compared to the pure and defective Cu(1 1 1) surface.

3.2. The adsorption of CH_x(x = 0–4) and H species on four different Cu surfaces

CH_4 dehydrogenation on different Cu surfaces leads to the formation of CH_x(x = 0–3) and H species. The adsorption energies of these species play an essential role in the CH_4 dehydrogenation. Thus, it is necessary to know the individual bonding natures of CH_x(x = 0–4) and H species on these surfaces, in which different adsorption sites have been considered. In this study, the adsorption energy (E_{ads}) is defined as the energy gain upon adsorption with respect to the substrates and the corresponding species in the gas phase. Here a negative value indicates that the adsorption is exothermic.

The most stable configurations for CH_4, CH_3, CH_2, CH, C and H obtained from our DFT calculations on Cu(1 1 1), Cu@Cu(1 1 1), RhCu(1 1 1), and Rh@Cu(1 1 1) surfaces are presented in Fig. 2, and the corresponding adsorption energies are listed in Table 1.

For CH_4 adsorption, on the flat Cu(1 1 1) or RhCu(1 1 1) surfaces, it favors to bind to the top Cu or the substituted Rh atoms, respectively; CH_4 molecule is 3.659 Å far away from the flat Cu(1 1 1) surface with only an adsorption of −19.0 kJ mol^{-1}. On Cu@Cu(1 1 1) or Rh@Cu(1 1 1) surfaces, CH_4 prefers to bind to the

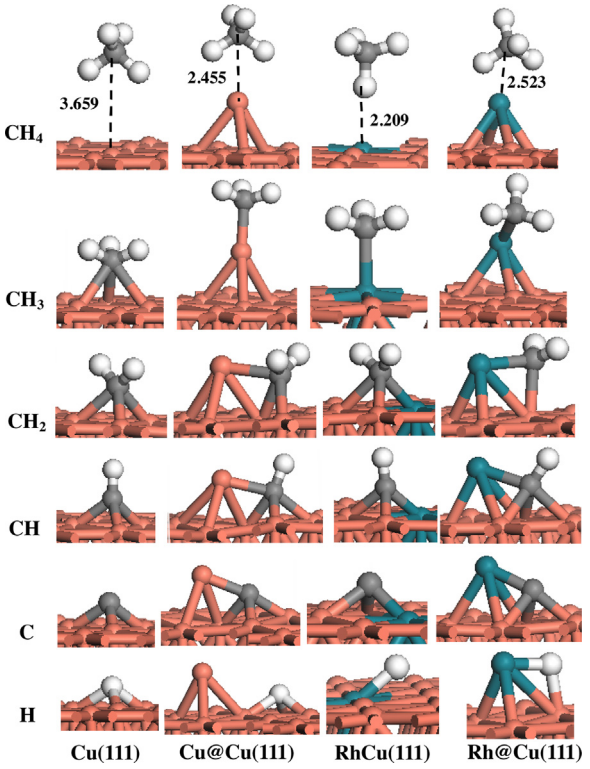

Fig. 2. The most stable configurations of CH_x(x = 0–4) and H species adsorbed on Cu(1 1 1), Cu@Cu(1 1 1), RhCu(1 1 1) and Rh@Cu(1 1 1) surfaces, respectively. Bond lengths are in Å. The C, H and Rh atoms are shown in the grey, white, and blue colors, respectively.

raised Cu or Rh adatom, the values of adsorption energy (−30.6 and −37.4 kJ mol^{-1}) indicate that CH_4 adsorption on Cu@Cu(111), RhCu(111) and Rh@Cu(111) is stronger than that on the pure Cu(111); moreover, CH_4 adsorption is a typical physisorption on these surfaces, this is because all the atoms in CH_4 are saturated in their coordinations, and the C – H bond has a low polarity. These results suggest that CH_4 prefers to adsorb at the raised metal atoms or the substituted Rh rather than Cu atoms on the flat surface.

For CH_3 adsorption, on Cu(1 1 1) surface, CH_3 favors to bind at the fcc site with an adsorption energy of −186.2 kJ mol^{-1}; on RhCu(1 1 1) surface, it prefers to adsorb at the surface Rh atom with the adsorption energy of −226.4 kJ mol^{-1}, which agrees with the studies by Zhao et al. [16]; on Cu@Cu(1 1 1) or Rh@Cu(1 1 1) surfaces, CH_3 favors to adsorb at the raised Cu or Rh adatom, the corresponding adsorption energies are −192.8 and −233.1 kJ mol^{-1}, respectively. Meanwhile, previous studies by Wang et al. [6] have shown that the adsorption site of CH_3 on Cu@Cu(1 0 0) or Ni@Cu(1 0 0) is also the raised Cu or Ni adatom. Further, the adsorption energy of CH_3 on Cu@Cu(1 1 1) is very near to the flat Cu(1 1 1) surface, and the differences are only 6.6 kJ mol^{-1}, suggesting that the morphology of Cu substrate does not obviously affect the adsorption of CH_3. However, CH_3 adsorption on RhCu(1 1 1) and Rh@Cu(1 1 1) surfaces are much stronger than those on Cu(1 1 1) and Cu@Cu(1 1 1) surfaces, indicating that the substituted or adsorbed Rh atom on RhCu(1 1 1) and Rh@Cu(1 1 1) surfaces are more reactive for CH_3 than the Cu atoms on Cu(1 1 1) and Cu@Cu(1 1 1) surfaces.

For CH_2 adsorption, on Cu(1 1 1) surface, CH_2 prefers to adsorb at the fcc site with the adsorption energy of −354.1 kJ mol^{-1}; on Cu@Cu(1 1 1) surface, CH_2 favors to bind at the three-fold hollow sites consisting of two surface Cu atoms and the raised Cu adatom, the corresponding adsorption energy is −345.0 kJ mol^{-1}; on RhCu(1 1 1) surface, it favors to bind to the fcc site around

Table 1
The adsorption energy of CH_x(x = 0–4) and H species for the most stable configurations adsorbed on Cu(1 1 1), Cu@Cu(1 1 1), RhCu(1 1 1), and Rh@Cu(1 1 1) surfaces, as well as the corresponding adsorption sites in parentheses.

Adsorbed species	Adsorption energy E_{ads}/kJ mol^{-1}			
	Cu(1 1 1)	Cu@Cu(1 1 1)	RhCu(1 1 1)	Rh@Cu(1 1 1)
CH_4	−19.0 (top)	−30.6 (raised Cu)	−24.0 (top Rh)	−37.4 (raised Rh)
CH_3	−186.2 (fcc)	−192.8 (raised Cu)	−226.4 (top Rh)	−233.1 (raised Rh)
CH_2	−354.1 (fcc)	−345.0 (3-fold site)	−397.7 (fcc)	−416.0 (Rh-Cu bridge)
CH	−524.6 (fcc)	−518.4 (4-fold site)	−584.0 (fcc)	−611.2 (4-fold site)
C	−496.5 (fcc)	−534.8 (4-fold site)	−599.4 (fcc)	−669.4 (4-fold site)
H	−273.0 (fcc)	−250.2 (fcc)	−299.5 (fcc)	−290.1(Rh-Cu bridge)

the Rh atom with an adsorption energy of −397.7 kJ mol^{-1}; on Rh@Cu(1 1 1) surface, CH_2 favors to adsorb at the Rh-Cu bridge site with an adsorption energy of −416.0 kJ mol^{-1}; meanwhile, previous DFT studies have shown that CH_2 is adsorbed at the Cu-Ni bridge site on Ni@Cu(1 0 0) surface [6]. Similarly, the adsorption energy on Cu@Cu(1 1 1) surface are very near to the flat Cu(1 1 1) surface, and CH_2 adsorption on RhCu(1 1 1) and Rh@Cu(1 1 1) surfaces are stronger than those on Cu(1 1 1) and Cu@Cu(1 1 1) surfaces.

For CH adsorption, on Cu(1 1 1) surface, CH prefers to adsorb at the fcc site with the adsorption energy of −524.6 kJ mol^{-1}; on Cu@Cu(1 1 1) surface, CH favors to bind at the four-fold hollow sites consisting of three surface Cu atoms and one raised Cu adatom, the corresponding adsorption energy is −518.4 kJ mol^{-1}; on Rh@Cu(1 1 1) surface, CH favors to adsorb at the four-fold hollow sites consisting of three surface Cu atoms and one raised Rh adatom with an adsorption energy of −584.0 kJ mol^{-1}, meanwhile, previous DFT studies have shown that CH is also adsorbed at the same site on Ni@Cu(1 0 0) surface [6]; on RhCu(1 1 1) surface, CH favors to bind at the fcc site around the Rh atom with the adsorption energy of −611.2 kJ mol^{-1}.

For atomic C adsorption, on Cu(1 1 1) surface, C prefers to adsorb at the fcc site with the adsorption energy of −496.5 kJ mol^{-1}; on Cu@Cu(1 1 1), similar to CH, C favors to bind at the four-fold hollow sites, the corresponding adsorption energy is −534.8 kJ mol^{-1}; on RhCu(1 1 1) surface, it favors to adsorb at the fcc sites with an adsorption energy of −599.4 kJ mol^{-1}; on Rh@Cu(1 1 1) surface, C favors to bind at the four-fold hollow sites, which consists of three surface Cu atoms and one raised Rh adatom with the adsorption energy of −669.4 kJ mol^{-1}.

For atomic H adsorption, on Cu(1 1 1), H prefers to adsorb at the fcc site with the adsorption energy of −273.0 kJ mol^{-1}, which is agreement with the values (−260.5 kJ mol^{-1}) obtained by Liao et al. [10]; on Cu@Cu(1 1 1), H favors to bind at the fcc site on the flat surface rather than the raised Cu atom, the corresponding adsorption energy is −250.2 kJ mol^{-1}; on RhCu(1 1 1), H favors to bind at the fcc site around the Rh atom, which has an adsorption energy of −299.5 kJ mol^{-1}; on Rh@Cu(1 1 1), it favors to adsorb at the Rh-Cu bridge site with an adsorption energy of −290.1 kJ mol^{-1}.

On the basis of above results, we can conclude that CH_4 adsorbed at four different Cu surfaces is typical of physisorption. However, CH_x(x = 0–3) and H species adsorbed on these surfaces is the strong chemisorption; moreover, all CH_x(x = 1–4) species prefers to bind with the adsorption site around the raised metal atoms or the substituted Rh rather than the only Cu atoms on the flat surface, suggesting that the successive dehydrogenation of CH_x(x = 1–4) species should have occurred around the raised metal adatom and the substituted Rh atom. The adsorption energies of CH_x(x = 1–4) species tend to increase with decreasing number of H atom, which was in good agreement with the other DFT studies [16,39]. Moreover, the adsorption of CH_x(x = 1–4) and H species on RhCu(1 1 1) and Rh@Cu(1 1 1) surfaces is much stronger than those on Cu(1 1 1) and Cu@Cu(1 1 1) surfaces, which means that the substituted or adsorbed Rh atom on RhCu(1 1 1) and Rh@Cu(1 1 1) surfaces are more reactive for CH_x(x = 1–4) species than Cu atoms on Cu(1 1 1) and Cu@Cu(1 1 1) surfaces, the differences in the adsorption energy of CH_x(x = 1–4) and H species is because the Rh − CH_x(H) interaction is stronger than Cu − CH_x(H) interaction; thus, the substituted or adsorbed Rh atom may exhibit good catalytic activity for CH_x(x = 1–4) species.

On the other hand, the adsorption energy of CH_x(x = 1–4) species on Cu@Cu(1 1 1) surface are very near to the flat Cu(1 1 1) surface, this suggests that the morphology of Cu substrate does not greatly affect the adsorption ability of CH_x(x = 1–4) species, which agrees with the previous DFT studies about the adsorption of CH_x(x = 1–4) species on Cu(1 0 0) and Cu@Cu(1 1 1) surfaces [6]; thus, we predicate that the catalytic behavior of CH_x(x = 1–4) species on Cu@Cu(1 1 1) surface may be the same with those on the flat Cu(1 1 1) surface.

3.3. Minimum energy path for CH_4 successive dehydrogenation

The reaction pathways and reaction energetic for the successive dehydrogenation of CH_4 to C and H on Cu(1 1 1), Cu@Cu(1 1 1), RhCu(1 1 1), and Rh@Cu(1 1 1) surfaces have been systematically studied using DFT analysis. Previous studies have shown the adsorption energy difference of CH_x fragment to the substrate caused by the removal of the dissociated H atom is slight on Cu(1 0 0) surface due to the small diffusion barrier of a single H atom [6], which is consistent with our results on Cu(1 1 1) surface, thus, the dissociated H in the final state of CH_x(x = 1–4) dehydrogenation to CH_{x-1}(x = 1–4) and H is removed in our study, and the remaining fragment CH_{x-1}(x = 2–4) is considered as the initial state of the next dehydrogenation step. The activation barrier and reaction energy of each dehydrogenation steps on different surfaces, the structures of initial state (IS), final state (FS), and transition state (TS), as well as the only one imaginary frequency corresponding to the transition state are presented in Figs. 3–6. A comparison between the reaction profiles on different Cu(1 1 1) surfaces is illustrated in Fig. 7.

For the reaction of $CH_x \rightarrow CH_{x-1} + H$ over different Cu(1 1 1) surfaces, the activation barrier (E_a) and reaction energy (ΔH) are calculated on the basis of the following formulas:

$$E_a = E_{TS} - E_{IS}$$
$$\Delta H = E_{FS} - E_{IS}$$

Where E_{IS} and E_{FS} are the total energies of different Cu(1 1 1) surfaces together with the adsorbed CH_x and the dissociated CH_{x-1} + H species, respectively; E_{TS} is the total energy of transition states for the reaction of $CH_x \rightarrow CH_{x-1}$ + H.

3.3.1. CH_4 Dehydrogenation

On the flat Cu(1 1 1), the first step of CH_4 dehydrogenation leads to the formations of CH_3 and H species, the co-adsorbed CH_3 fragment and H adatom employed as the FS4-1 configuration are adsorbed at the bridge and fcc sites, respectively. This FS4-1 configuration is in good agreement with the previous studies [4]. As shown in Fig. 3, the dissociated H atom directly moves to the fcc site via a transition state TS4-1; in TS4-1, H adatom is adsorbed at

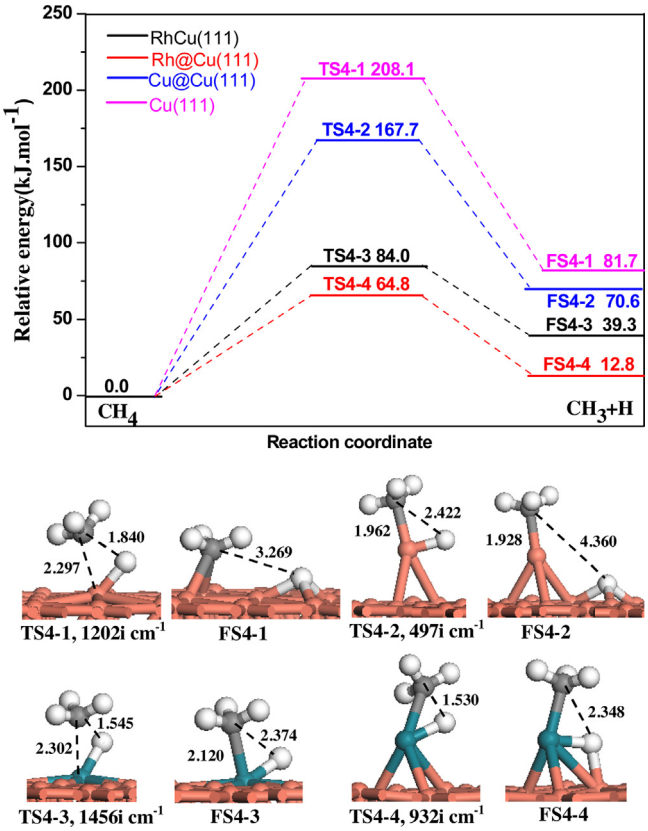

Fig. 3. The potential energy diagram for CH_4 dehydrogenation to CH_3 + H species on different Cu(1 1 1) surfaces together with final states (FSs) and transition states (TSs), as well as the only one imaginary frequency corresponding to TSs. Bond lengths are in Å. See Fig. 2 for color coding.

the top Cu atom; this elementary reaction has an activation barrier of 208.1 kJ mol^{-1}, it is endothermic by 81.7 kJ mol^{-1}.

In the case of Cu(1 1 1) surface with a Cu or Rh adatom, the raised metal atom is acted as the reaction active center, where the dissociated CH_3 fragment prefers to chemisorb at the raised Cu or Rh adatom. This dehydrogenation step involves the transition states TS4-2 and TS4-4, respectively, in which the dissociated H atom binds at the raised Cu or Rh adatom. In FS4-2 and FS4-4, H adatom prefers to chemisorb at the fcc site of the flat surface and the Rh–Cu bridge site, respectively. The activation barriers of CH_4 dehydrogenation on Cu@Cu(1 1 1) and Rh@Cu(1 1 1) surfaces are 167.7 and 64.8 kJ mol^{-1}, respectively; the corresponding reaction energy are 70.6 and 12.8 kJ mol^{-1}, respectively.

On RhCu(1 1 1) surface, both the dissociated CH_3 fragment and H adatom prefer to chemisorb at the raised Rh atom and the Rh–Cu bridge site, respectively, this step goes through the transition state TS4-3. The activation barrier is 84.0 kJ mol^{-1} with the reaction energy of 39.3 kJ mol^{-1}.

Above results show that Rh@Cu(1 1 1) and RhCu(1 1 1) surfaces with the adsorbed and substituted Rh atom can exhibit good catalytic activity for CH_4 dehydrogenation to CH_3 + H species compared to the Cu@Cu(1 1 1) and the flat Cu(1 1 1) surfaces.

3.3.2. CH_3 Dehydrogenation

On the flat Cu(1 1 1), CH_3 adsorbed at the fcc site is selected as the initial state, the co-adsorbed configuration of CH_2 fragment at the fcc site and H adatom at the fcc site is employed as the final state FS3-1, as presented in Fig. 4. CH_3 dehydrogenation leads to CH_2 and H species via the transition state TS3-1, the dissociated H atom adsorbs at the top site in TS3-1, then, it moves to the fcc site; this dehydrogenation step has an activation barrier of 166.0 kJ mol^{-1}, it is endothermic by 83.3 kJ mol^{-1}.

On Cu@Cu(1 1 1) surface, starting from CH_3, CH_3 dehydrogenation firstly goes through TS3-2 to form an intermediate IM3, in which the dissociated H atom is adsorbed at the Cu–Cu bridge site of the tetrahedron; this elementary step has a much higher activation barrier of 223.9 kJ mol^{-1} with the reaction energy of 78.2 kJ mol^{-1}. Subsequently, the dissociated H atom in IM3 migrates from the Cu–Cu bridge to the fcc site over the flat Cu surface via the transition state TS3-2′, this elementary step has only an activation barrier of 23.7 kJ mol^{-1}, it is endothermic by 11.1 kJ mol^{-1}. Since the interaction of H adsorbed at the fcc site of the flat surface is relatively stronger than the interaction of H adsorbed at the Cu–Cu bridge site of the tetrahedron, H atom always takes the favorable adsorption site to obtain the most stable adsorption configuration.

On RhCu(1 1 1) surface, the substituted Rh atom is acted as the active center; CH_3 species adsorbed at the Rh atom is selected as the initial state, the dissociated H atom directly moves to the fcc site via TS3-3; the dissociated CH_2 fragment is chemisorbed at the fcc site; this step is endothermic by 53.0 kJ mol^{-1} with an activation barrier of 112.6 kJ mol^{-1}.

On Rh@Cu(1 1 1) surface, the raised Rh atom is acted as the reaction center; beginning with CH_3 species adsorbed at the raised Rh atom, CH_3 can dehydrogenate to CH_2 + H species via TS3-4, in the final state FS3-4, the dissociated H atom and CH_2 fragment are adsorbed at two adjacent Rh-Cu bridge sties of the tetrahedron; this elementary step has an activation barrier of 121.6 kJ mol^{-1}, it is endothermic by 41.3 kJ mol^{-1}.

Above results show that Rh@Cu(1 1 1) and RhCu(1 1 1) surfaces would be the most active for catalyzing CH_3 dehydrogenation, with Cu@Cu(1 1 1) surface the least active; namely, the adsorbed or substituted Rh atom over the flat Cu(1 1 1) surface can still exhibit good catalytic activity for CH_3 dehydrogenation compared to the Cu@Cu(1 1 1) and the flat Cu(1 1 1) surfaces.

3.3.3. CH_2 Dehydrogenation

In the case of the flat Cu(1 1 1), CH_2 adsorbed at the fcc site is selected as the initial state, which can dehydrogenate via the transition state TS2-1 into the final state FS2-1, CH + H species; in TS2-1, the dissociated H atom is adsorbed at the top Cu atom; in FS2-1, CH and H species are adsorbed at two adjacent fcc sites; this dehydrogenation step has an activation barrier of 125.2 kJ mol^{-1}, it is endothermic by 61.5 kJ mol^{-1}.

On Cu@Cu(1 1 1) surface, CH_2 favors to bind at the three-fold hollow sites consisting of two surface Cu atoms and the raised Cu adatom, CH_2 dehydrogenation leads to the final state FS2-2 of CH + H species via TS2-2; in TS2-2, the dissociated H atom is adsorbed at the Cu atom of the flat surface, CH is adsorbed at the three-fold hollow sites consisting of two surface Cu atoms and one raised Cu adatom; in FS2-2, CH favors to bind at the four-fold hollow sites consisting of three surface Cu atoms and one raised Cu adatom, the dissociated H atom is adsorbed at the fcc site of the flat surface; this dehydrogenation step has a higher activation barrier of 146.9 kJ mol^{-1} with the reaction energy of 53.6 kJ mol^{-1}.

On RhCu(1 1 1) surface, CH_2 favors to adsorb at the fcc site around the Rh atom; CH_2 dehydrogenates into CH + H species via TS2-3; in FS2-3, both the dissociated CH fragment and H atom prefer to bind at two adjacent fcc site around Rh atom. Thus, the substituted Rh atom is acted as the active center; the activation barrier of this dehydrogenation step is 93.8 kJ mol^{-1}, it is endothermic by 22.3 kJ mol^{-1}.

In the case of Rh@Cu(1 1 1) surface, CH_2 favors to adsorb at the Rh-Cu bridge site employed as the initial state; in FS2-4, the dissociated CH fragment prefers to adsorb at the four-fold hollow sites consisting of three surface Cu atoms and one raised Rh

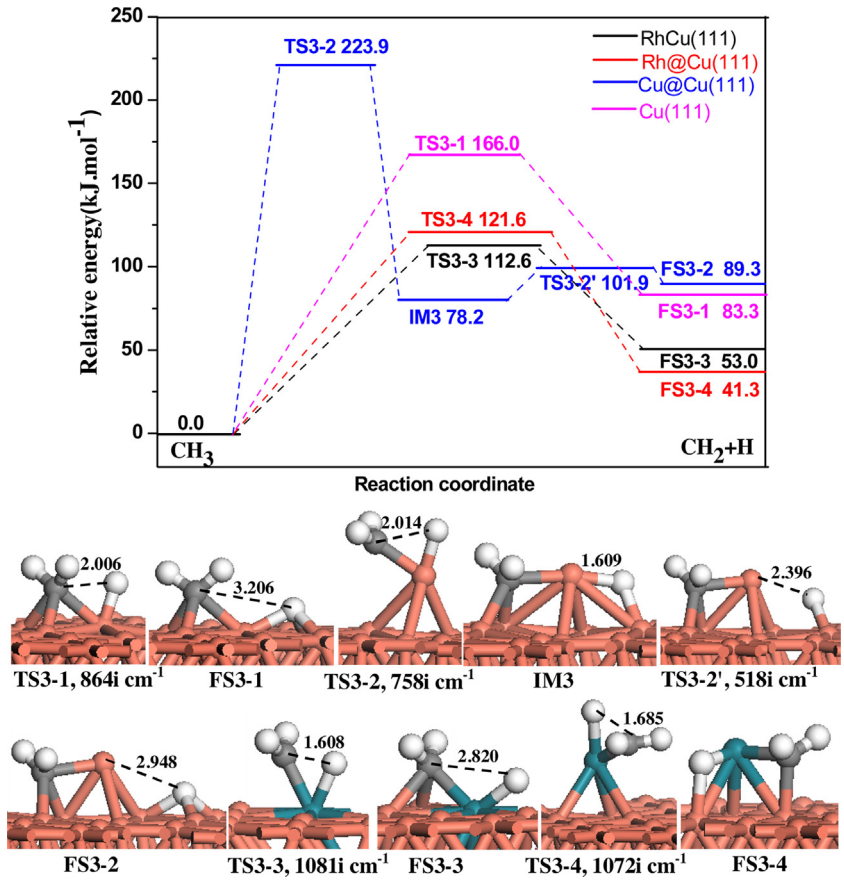

Fig. 4. The potential energy diagram for CH_3 dehydrogenation to CH_2 + H species on different Cu(1 1 1) surfaces together with FSs and TSs, as well as the only one imaginary frequency corresponding to TSs. Bond lengths are in Å. See Fig. 2 for color coding.

adatom, and the dissociated H is located at the raised Rh atom. This dehydrogenation step involves the transition states TS2-4 with the activation barrier and reaction energy of 125.9 and 4.7 kJ mol^{-1}, respectively; similarly, the raised Rh atom is acted as the active center.

As shown in Fig. 5, RhCu(1 1 1) surface would be the most active for catalyzing CH_2 dehydrogenation, with Cu@Cu(1 1 1) surface the least active; namely, the substituted Rh atom over the flat Cu(1 1 1) surface can exhibit good catalytic activity for CH_2 dehydrogenation compared to another three Cu(1 1 1) surfaces.

3.3.4. CH dehydrogenation

On the flat Cu(1 1 1), CH adsorbed at the fcc site is selected as the initial state, the co-adsorbed configuration of C at the fcc site and H adatom at the hcp site is employed as the final state FS1-1, as seen in Fig. 6. CH dehydrogenation leads to C and H species via TS1-1, this step has a much higher activation barrier of 222.2 kJ mol^{-1}, it is strongly endothermic by 137.3 kJ mol^{-1}.

On Cu@Cu(1 1 1) surface, CH adsorbed at the four-fold hollow sites consisting of three surface Cu atoms and one raised Cu adatom is selected as the initial state, CH dehydrogenates via TS1-2 to FS1-2, in which the dissociated H atom is still adsorbed at the four-fold hollow sites and H atom is located at the fcc site on the flat surface; this elementary step has a higher activation barrier of 204.9 kJ mol^{-1} with the reaction energy of 105.1 kJ mol^{-1}.

On RhCu(1 1 1) surface, CH adsorbed at the fcc site around the Rh atom can dehydrogenate into C + H species via TS1-3; the dissociated C and H adatom are chemisorbed at the fcc and hcp sites, respectively. This step has an activation barrier of 144.3 kJ mol^{-1}, it is endothermic by 70.0 kJ mol^{-1}.

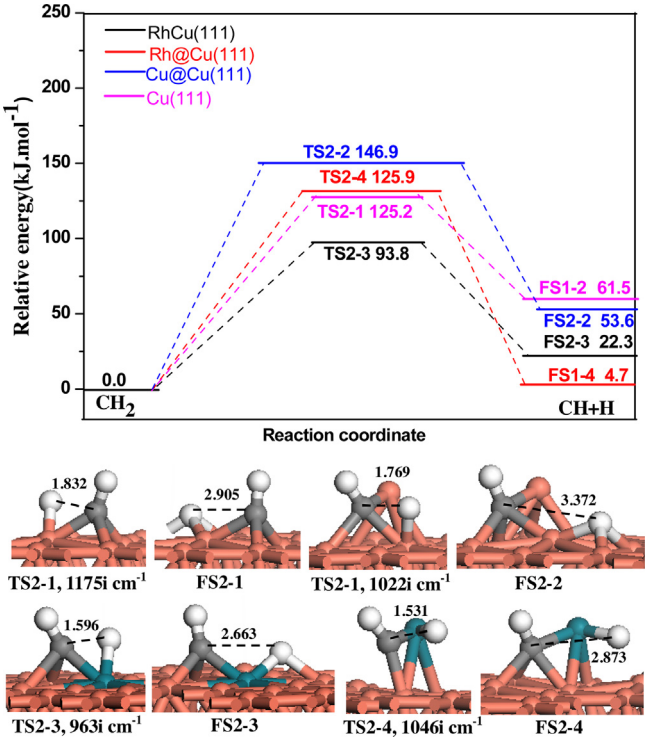

Fig. 5. The potential energy diagram for CH_2 dehydrogenation to CH + H species on different Cu(111) surfaces together with FSs and TSs, as well as the only one imaginary frequency corresponding to TSs. Bond lengths are in Å. See Fig. 2 for color coding.

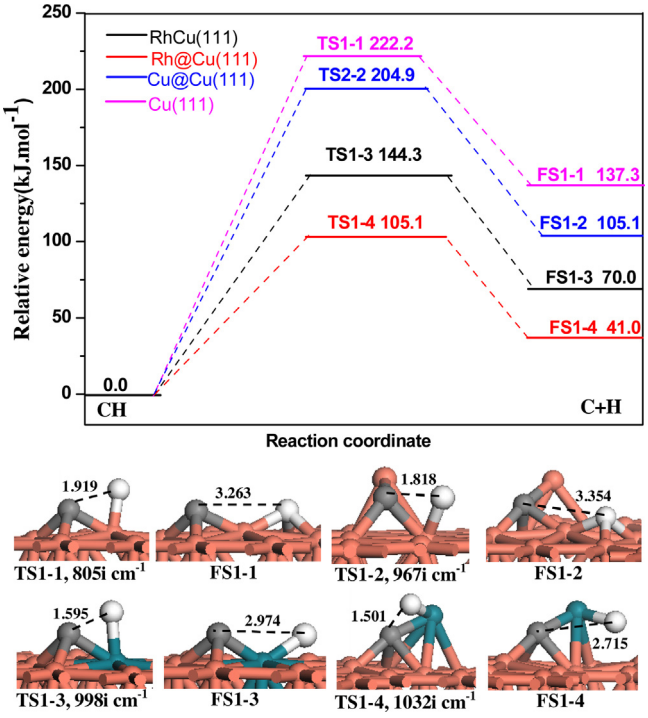

Fig. 6. The potential energy diagram for CH dehydrogenation to C + H species on different Cu(1 1 1) surfaces together with FSs and TSs, as well as the only one imaginary frequency corresponding to TSs. Bond lengths are in Å. See Fig. 2 for color coding.

On Rh@Cu(1 1 1) surface, CH prefers to adsorb at the four-fold hollow sites consisting of three surface Cu atoms and one raised Rh adatom; CH can dehydrogenate to C + H species via TS1-4; in FS1-4, the dissociated H and C atoms are adsorbed at the four-fold hollow sites and the raised Rh atom, respectively; This dehydrogenation step has an activation barrier of 105.1 kJ mol^{-1}, it is endothermic by 41.0 kJ mol^{-1}.

Above results show that Rh@Cu(1 1 1) surface would be the most active for catalyzing CH dehydrogenation, in which the adsorbed Rh atom over the flat Cu(1 1 1) surface can exhibit good catalytic activity.

3.4. General discussions

Aiming at illustrating the similarities and differences of CH_4 complete dehydrogenation among four types of Cu(1 1 1) surfaces, the potential energy profiles in Fig. 7 presents all the elementary steps involved in CH_x(x = 1–4) dehydrogenation on different types of Cu(1 1 1) surfaces.

As shown in Fig. 7, the reaction energies of CH_4 complete dehydrogenation are 363.8, 318.6, 184.6 and 99.8 kJ mol^{-1} on Cu(1 1 1), Cu@Cu(1 1 1), RhCu(1 1 1) and Rh@Cu(1 1 1) surfaces, respectively; meanwhile, all dehydrogenation steps on four different surfaces are endothermic. However, in gas phase, previous studies [40] have shown that CH_4 sequential dehydrogenation is endothermic, and the computed reaction energies are 457.3, 479.5, 479.5 and 350.2 kJ mol^{-1} for each dehydrogenation step, which means that a total of 1766.5 kJ mol^{-1} is needed for CH_4 complete dehydrogenation. Comparatively, CH_4 complete dehydrogenation on four different Cu(1 1 1) surfaces is much more favorable thermodynamically. On the basis of reaction energies, we can obtain that the reaction energy of CH_4 complete dehydrogenation on Rh@Cu(1 1 1) surface is remarkably reduced to 99.8 kJ mol^{-1}; namely, in view of the thermodynamics, Rh@Cu(1 1 1) is the most favorable surface for CH_4 complete dehydrogenation, followed by RhCu(1 1 1), Cu@Cu(1 1 1), and Cu(1 1 1) surfaces.

On Cu(1 1 1) surface, the last step CH→C + H is the rate-limiting step for CH_4 complete dehydrogenation with an activation barrier of 222.2 kJ mol^{-1}; On Cu@Cu(1 1 1) surface, the second step CH_3→CH_2 + H turns out to be the rate-limiting step with an activation barrier of 223.9 kJ mol^{-1}; However, on RhCu(1 1 1) surface, the rate-limiting step becomes the last step CH→C + H, and the corresponding activation barrier is obviously reduced to 144.3 kJ mol^{-1}; on Rh@Cu(1 1 1) surface, the third step CH_2→CH + H is the rate-limiting step, the activation barrier is strongly reduced to 125.9 kJ mol^{-1}; On the other hand, as shown in Fig. 7, with respect to CH_4 adsorption on different Cu(1 1 1) surfaces, we can see that the highest barrier and reaction energy are 448.7 and 363.8 kJ mol^{-1} on Cu(1 1 1) surface, respectively; on Cu@Cu(1 1 1) surface, the highest barrier and reaction energy are 418.4 and 318.6 kJ mol^{-1}, respectively; on RhCu(1 1 1) surface, the highest barrier and reaction energy are 258.9 and 184.6 kJ mol^{-1}, respectively; whereas, on Rh@Cu(1 1 1) surface, the highest barrier and reaction energy are remarkably reduced to 180.0 and 99.8 kJ mol^{-1}, respectively; Therefore, above thermodynamic and kinetic results suggest that CH_4 dissociation on Rh@Cu(1 1 1) surface is the most favorable both thermodynamically and kinetically in comparison to those on Cu(1 1 1), Cu@Cu(1 1 1) and RhCu(1 1 1) surfaces, namely, Rh@Cu(1 1 1) is the most favorable surface for CH_4 dehydrogenation.

As mentioned above, for CH_4 complete dehydrogenation on the pure Cu catalyst, the catalytic activity of Cu@Cu(1 1 1) surface are

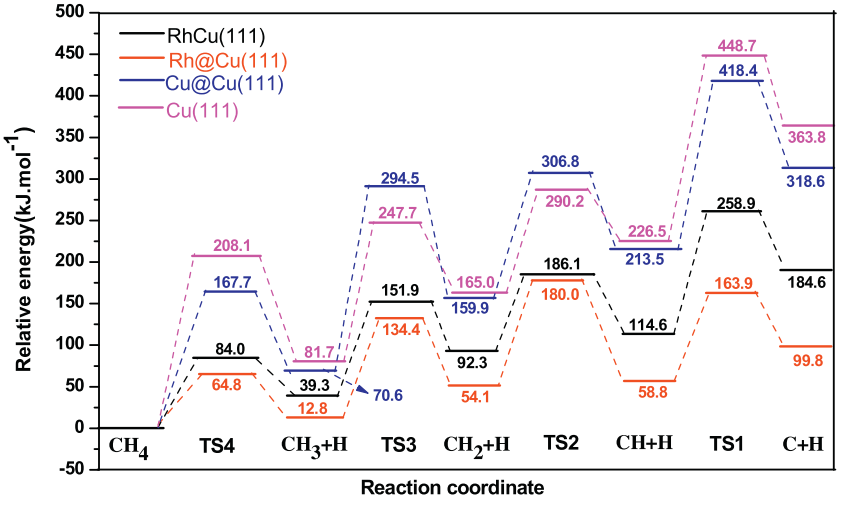

Fig. 7. The potential energy profiles of CH_4 complete dehydrogenation on Cu(1 1 1), Cu@Cu(1 1 1), RhCu(1 1 1), and Rh@Cu(1 1 1) surfaces.

very similar to the flat Cu(1 1 1) surface; the differences of the highest barriers and reaction energy are smaller than 46.0 kJ mol^{-1}; our results are in agreement with the previous studies about CH_4 complete dehydrogenation on Cu@Cu(1 0 0) and the flat Cu(1 0 0) surfaces, in which the corresponding highest barriers and reaction energy are smaller than 29.0 kJ mol^{-1} [6]. These results indicate that the morphology of the pure Cu catalyst does not remarkably affect the catalytic activity of CH_4 complete dehydrogenation and the nucleation position of grapheme growth; moreover, the experimental observations using scanning tunneling microscopy have revealed that the growth of macroscopic pristine graphene is not limited by the underlying copper structure including the atomically flat planes, monatomic steps, edges, and vertices of the copper surface [41]. As a result, taking the previous studies about Cu(1 0 0) into consideration, we can obtain that the Cu adatom is just like the other Cu atoms in the flat Cu(1 1 1) and (1 0 0) surfaces, which is not served as the specific active center; thus, Cu@Cu(1 1 1) and Cu@Cu(100) surfaces exhibit the same catalytic activity as the corresponding flat Cu(1 1 1) and Cu(1 0 0) surfaces, which agrees with the experimental facts that both Cu(1 0 0) and (1 1 1) surfaces can promote the CVD growth of graphene [26,27].

On the basis of above analysis, compared to the flat Cu surface, Rh@Cu(1 1 1) surface greatly reduces the highest barriers by about 60% for CH_4 complete dehydrogenation, all the CH_x dehydrogenation steps on Rh@Cu(1 1 1) are modestly endothermic, which means that Rh@Cu(1 1 1) exhibits a high catalytic activity toward CH_4 complete dehydrogenation, further the graphene growth. Moreover, the adsorbed Rh atom is the active reaction center, namely, the adsorbed Rh atom is the graphene nucleation position, thus, by manipulating the graphene nucleation position, the CVD growth of graphene may be controlled; Further, Sinfelt et al. have experimentally obtained the Rh-Cu bimetallic samples by the extended X-ray absorption fine structure (EXAFS) technique, and presented an apparent enrichment of copper on the surface but little miscibility in the bulk of Rh-Cu clusters [42], then, the Rh-Cu catalyst has been reported as an efficient system for NO reduction by CO, the conversion of methane to ethane, and some dehydrogenation reactions [18,43,44], suggesting that the synthesis for the dilute-Rh adsorbed Cu alloy foils is possible, which may be employed as the excellent catalyst to control the CVD growth of graphene.

Finally, our present studies suggest that the promoter Rh-decorated Cu catalyst can greatly improve the catalytic activity toward CH_4 complete dehydrogenation, further the CVD growth of graphene from CH_4, namely, promoter Rh is a promising candidate for an improved catalyst of the graphene CVD growth. More importantly, the understanding about the effect of promoter Rh on the catalytic activity of CH_4 dehydrogenation over Cu-based catalyst at the atomic level, which can potentially be applied to develop and design the more superior Cu-based catalysts for the graphene CVD growth from CH_4 by probing into more effective other promoter metals, this is beyond the scope of the present study, which will be discussed in our next work.

4. Conclusions

In this study, aiming at illustrating the effects of Cu morphology and promoters on the catalytic activity of the graphene CVD growth from CH_4, four types of Cu(1 1 1) surfaces, the flat Cu(1 1 1), RhCu(1 1 1), Cu@Cu(1 1 1) and Rh@Cu(1 1 1), have been employed to investigated CH_4 complete dehydrogenation at the atomic level by using density functional theory method. Our results show that compared to the pure Cu catalyst, the promoter Rh-decorated Cu catalyst, especially Rh-adsorbed Cu catalyst, can greatly improve the catalytic activity toward CH_4 dehydrogenation; the highest barrier and reaction energy on Rh-adsorbed Cu catalyst are remarkably reduced to 180.0 and 99.8 kJ mol^{-1} from 448.7 and 363.8 kJ mol^{-1} on Cu(1 1 1) surface, as well as 418.4 and 318.6 kJ mol^{-1} Cu@Cu(1 1 1) surface, respectively; namely, Rh@Cu(1 1 1) is the most favorable surface both thermodynamically and kinetically for CH_4 complete dehydrogenation. Moreover, the adsorbed Rh atom is the active reaction center and the graphene nucleation position, as a result, by manipulating activation reaction center, the CVD growth of graphene may be controlled. Further, our calculations show that active promoter atom into inactive Cu substrate can exhibit good catalytic activity and is a promising candidate for an improved catalyst of the graphene CVD growth, which may be make the graphene CVD growth occur at relatively low temperature.

Acknowledgments

This work is financially supported by the National Natural Science Foundation of China (No. 21276003, 21476155 and 21276171), the Natural Science Foundation of Shanxi Province (No. 2014011012-2), the State Key Laboratory of Fine Chemicals (KF1205), the Program for the Top Young Academic Leaders of Higher Learning Institutions of Shanxi, and the Top Young Innovative Talents of Shanxi.

References

[1] K.S. Kim, Y. Zhao, H. Jang, S.Y. Lee, J.M. Kim, K.S. Kim, J.H. Ahn, P. Kim, J.Y. Choi, B.H. Hong, Large-scale pattern growth of graphene films for stretchable transparent electrodes, Nature 457 (2009) 706–710.
[2] X.S. Li, W.W. Cai, J.H. An, S. Kim, J. Nah, D.X. Yang, R. Piner, A. Velamakanni, I. Jung, E. Tutuc, S.K. Banerjee, L. Colombo, R.S. Ruoff, Large-area synthesis of high-quality and uniform graphene films on copper foils, Science 324 (2009) 1312–1314.
[3] A.N. Obraztsov, Chemical vapour deposition: making graphene on a large scale, Nat. Nanotechnol. 4 (2009) 212–213.
[4] W.H. Zhang, P. Wu, Z. Li, J.L. Yang, First-principles thermodynamics of graphene growth on Cu surfaces, J. Phys. Chem. C 115 (2011) 17782–17787.
[5] X.S. Li, W.W. Cai, L. Colombo, R.S. Ruoff, Evolution of graphene growth on Ni and Cu by carbon isotope labeling, Nano Lett. 9 (2009) 4268–4272.
[6] S.J. Yuan, L.J. Meng, J.L. Wang, Greatly improved methane dehydrogenation via Ni adsorbed Cu(100) surface, J. Phys. Chem. C 117 (2013) 14796–14803.
[7] X. Zhu, D.G. Cheng, P.Y. Kuai, Catalytic decomposition of methane over Ni/Al_2O_3 catalysts: effect of plasma treatment on carbon formation, Energy Fuels 22 (2008) 1480–1484.
[8] J.G. Li, E. Croiset, L. Ricardez-Sandoval, Methane dissociation on Ni(100), Ni(111), and Ni(553): A comparative density functional theory study, J. Mol. Catal. A Chem. 365 (2012) 103–114.
[9] B. Xing, X.Y. Pang, G.C. Wang, C-H bond activation of methane on clean and oxygen pre-covered metals: A systematic theoretical study, J. Catal. 282 (2013) 74–82.
[10] M.S. Liao, C.T. Au, C.F. Ng, Methane dissociation on Ni, Pd, Pt and Cu metal (111) surfaces-A theoretical comparative study, Chem. Phys. Lett. 272 (1997) 445–452.
[11] A. Kokalj, N. Bonini, S. de Gironcoli, C. Sbraccia, G. Fratesi, S. Baroni, Methane dehydrogenation on Rh@Cu(111): A first principles study of a model catalyst, J. Am. Chem. Soc. 128 (2006) 12448–12454.
[12] J.H. Larsen, I. Chorkendorff, Increased dissociation probability of CH_4 on Co/Cu(111), Surf. Sci. 405 (1998) 62–73.
[13] W. An, X.C. Zeng, C.H. Turner, First-principles study of methane dehydrogenation on a bimetallic Cu/Ni(111) surface, J. Chem. Phys. 131 (2009) 174702.
[14] Y.H. Zhao, S.G. Li, Y.H. Sun, Theoretical study on the dissociative adsorption of CH_4 on Pd-doped Ni surfaces, Chin. J. Catal. 34 (2013) 911–922.
[15] R.G. Zhang, G.R. Wang, B.J. Wang, Insights into the mechanism of ethanol formation from syngas on Cu and an expanded prediction of improved Cu-based catalyst, J. Catal. 305 (2013) 238–255.
[16] Y.H. Zhao, M.M. Yang, D.P. Sun, H.Y. Su, K.J. Sun, X.F. Ma, X.H. Bao, W.X. Li, Rh-decorated Cu alloy catalyst for improved C_2 oxygenate formation from syngas, J. Phys. Chem. C 115 (2011) 18247–18256.
[17] S. González, D. Loffreda, P. Sautet, F. Illas, Theoretical study of no dissociation on stepped Rh(221) and RhCu(221) surfaces, J. Phys. Chem. C 111 (2007) 11376–11383.
[18] F. Solymosi, J. Cserenyi, Enhanced formation of ethane in the conversion of methane over Cu-Rh/SiO_2, Catal. Let. 34 (1995) 343–350.
[19] B. Delley, An all-electron numerical method for solving the local density functional for polyatomic molecules, J. Chem. Phys. 92 (1990) 508–517.
[20] B. Delley, From molecules to solids with the DMol^3 approach, J. Chem. Phys. 113 (2000) 7756–7764.

[21] J.P. Perdew, Y. Wang, Accurate and simple analytic representation of the electron-gas correlation energy, Phys. Rev. B 45 (1992) 13244–13249.
[22] P. Hohenberg, W. Kohn, Inhomogeneous electron gas, Phys. Rev. B 136 (1964) B864–B871.
[23] M. Dolg, U. Wedig, H. Stoll, H. Preuss, Energy-adjusted ab initio pseudopotentials for the first row transition elements, J. Chem. Phys. 86 (1987) 866–872.
[24] A. Bergner, M. Dolg, W. Kuechle, H. Stoll, H. Preuss, Ab initio energy-adjusted pseudopotentials for elements of groups 13-17, Mol. Phys. 80 (1993) 1431–1441.
[25] T.A. Halgren, W.N. Lipscomb, The synchronous-transit method for determining reaction pathways and locating molecular transition states, Chem. Phys. Lett. 49 (1977) 225–232.
[26] J.M. Wofford, S. Nie, K.F. McCarty, N.C. Bartelt, O.D. Dubon, Graphene islands on Cu foils: The interplay between shape, orientation, and defects, Nano Lett. 10 (2010) 4890–4896.
[27] H. Kim, C. Mattevi, M.R. Calvo, J.C. Oberg, L. Artiglia, S. Agnoli, C.F. Hirjibehedin, M. Chhowalla, E. Saiz, Activation energy paths for graphene nucleation and growth on Cu, ACS Nano 6 (2012) 3614–3623.
[28] L.C. Grabow, M. Mavrikakis, Mechanism of methanol synthesis on Cu through CO_2 and CO hydrogenation, ACS Catal. 1 (2011) 365–384.
[29] Z.P. Liu, P. Hu, General rules for predicting where a catalytic reaction should occur on metal surfaces: A density functional theory study of C-H and C-O bond breaking/making on flat, stepped, and kinked metal surfaces, J. Am. Chem. Soc. 125 (2003) 1958–1967.
[30] A.A. Gokhale, J.A. Dumesic, M. Mavrikakis, On the mechanism of low-temperature water gas shift reaction on copper, J. Am. Chem. Soc. 130 (2008) 1402–1414.
[31] P. Ferrin, M. Mavrikakis, Structure sensitivity of methanol electrooxidation on transition metals, J. Am. Chem. Soc. 131 (2009) 14381.
[32] M. Behrens, F. Studt, I. Kasatkin, S. Kühl, M. Hävecker, F. Abild-Pedersen, S. Zander, F. Girgsdies, P. Kurr, B.L. Kniep, M. Tovar, R.W. Fischer, J.K. Nørskov, R. Schlögl, The active site of methanol synthesis over $Cu/ZnO/Al_2O_3$ industrial catalysts, Science 336 (2012) 893–897.
[33] H.F. Wang, Z.P. Liu, Selectivity of direct ethanol fuel cell dictated by a unique partial oxidation channel, J. Phys. Chem. C Lett. 111 (2007) 12157–12160.
[34] Y.X. Yang, M.G. White, P. Liu, Theoretical study of methanol synthesis from CO_2 hydrogenation on metal-doped Cu(111) surfaces, J. Phys. Chem. C 116 (2012) 248–256.
[35] M. Li, W.Y. Guo, R.B. Jiang, L.M. Zhao, X.Q. Lu, H.Y. Zhu, D.L. Fu, H.G. Shan, Density functional study of ethanol decomposition on Rh(111), J. Phys. Chem. C 114 (2010) 21493–21503.
[36] M. Li, W.Y. Guo, R.B. Jiang, L.M. Zhao, H.H. Shan, Decomposition of ethanol on Pd(111): A density functional theory study, Langmuir 26 (2010) 1879–1888.
[37] Y.M. Choi, P. Liu, Mechanism of ethanol synthesis from syngas on Rh(111), J. Am. Chem. Soc. 131 (2009) 13054–13061.
[38] D.R. Lide (Ed.), CRC Handbook of Chemistry and Physics, 76th ed., CRC Press, Boca Raton, FL, 1996.
[39] R.G. Zhang, L.Z. Song, Y.H. Wang, Insight into the adsorption and dissociation of CH_4 on Pt(hkl) surfaces: A theoretical study, Appl. Surf. Sci. 258 (2012) 7154–7160.
[40] S.G. Wang, D.B. Cao, Y.W. Li, J.G. Wang, H.J. Jiao, CH_4 dissociation on Ni surfaces: density functional theory study, Surf. Sci. 600 (2006) 3226–3234.
[41] H.I. Rasool, E.B. Song, M.J. Allen, J.K. Wassei, R.B. Kaner, K.L. Wang, B.H. Weiller, J.K. Gimzewski, Continuity of graphene on polycrystalline copper, Nano Lett. 11 (2011) 251–256.
[42] G. Meitzner, G.H. Via, F.W. Lytle, J.H. Sinfelt, Structure of Bi-metallic clusters. Extended x-ray absorption fine structure (EXAFS) studies of Rh-Cu clusters, J. Chem. Phys. 78 (1983) 882–889.
[43] L. Petrov, J. Soria, L. Dimitrov, R. Cataluna, L. Spasov, P. Dimitrov, Cu exchanged microporous titanium silicalite (TS-1) coated on polycrystalline mullite fibres as catalyst for the CO and NO conversion, Appl. Catal. B: Environ. 8 (1996) 9–31.
[44] P. Reyes, G. Pecchi, J.L.G. Fierro, Surface structures of Rh–Cu sol–gel catalysts and performance for crotonaldehyde hydrogenation, Langmuir 17 (2001) 522–527.